

Characteristic scaling parameters for tunneling in strong time-dependent electric fields

Mathias Wagner*

Hitachi Cambridge Laboratory, Madingley Road, Cambridge CB3 0HE, United Kingdom
and Universität München, Sektion Physik, Theresienstraße 37, D-80333 München, Germany

W. Zwerger

Universität München, Sektion Physik, Theresienstraße 37, D-80333 München, Germany

(Received 23 December 1996)

Tunneling through a single driven barrier is studied where the ac potential on either side of the barrier is of the general form $V_{ac}(z,t) = (\hat{a}^{l,r}z + \hat{b}^{l,r})\cos\omega t$ (l,r : left,right). Analytic expressions for the transmission and reflection amplitudes are obtained in the δ -barrier limit. The ω^{-1} characteristic scaling behavior of the Tien-Gordon theory is recovered in the special case of *vanishing* ac fields, $\hat{a}^{l,r} = 0$, while an ω^{-2} scaling is found for *finite* ac fields, $\hat{a}^{l,r} \neq 0$, which is *not* contained in the Tien-Gordon theory. An analogy with the Fabry-Perot interferometer is used to extend the theory to multiple barriers. Implications for experiments are discussed. [S0163-1829(97)50916-7]

Atoms exposed to intense time-dependent electric fields have been the subject of interest for some two decades (see, for instance, the reviews in Ref. 1), but only recently have technological advances made it possible to study artificial nanostructures in intense driving fields. By engineering the confinement potential and the band structure, photon-assisted tunneling (PAT) is now being investigated in a wealth of different driven systems, such as quantum point contacts² and quantum dots^{3,4} with ac voltages fed to the gates, superlattices exposed to free-electron lasers,⁵⁻⁷ and resonant tunneling diodes subjected to THz frequencies.⁸ Much of the analysis of these experiments is based on the theories by Tien-Gordon⁹ and Tucker,¹⁰ developed for tunneling through a *single* barrier, where the collector side has a *spatially uniform* ac potential $V_{ac}\cos\omega t$ superimposed on it. Essentially, these theories predict “photonic” sidebands in the transmission probability, due to multiple photon emission and absorption, with amplitudes proportional to $J_n^2(b)$, where J_n is the Bessel function of the first kind, n the sideband index, and $b = V_{ac}/\hbar\omega$ the characteristic scaling of the driving ac potential. However, in most experiments the ac potential does vary in space, and hence the applicability of the Tien-Gordon-Tucker theory is in doubt.

To address this point we study in the present paper the characteristic scaling properties of PAT in ac potentials that depend on the spatial coordinate. In particular, we show how the $V_{ac}/\hbar\omega$ scaling parameter of the Tien-Gordon theory relates to the recently discussed ω^{-2} scaling found in isolated quantum wells driven with $V_{ac}(z,t) = eFz\cos\omega t$.^{11,12} The polarization and spatial behavior of the ac field is shown to have a profound impact on the characteristic scaling of PAT, which is highly relevant to experimental designs.

Various transfer-matrix techniques have been used to calculate the transmission and reflection probabilities for driven tunneling structures.¹³⁻¹⁵ Here we take advantage of an analogy with optics and introduce a Fabry-Perot approach to tunneling in driven systems which, so far, has only been applied to static double-barrier diodes.¹⁶ The main conceptual advan-

tage of this approach is that one reduces the complex problem of tunneling through a multiple-barrier heterostructure to that of finding the transmission and reflection amplitudes of single driven barriers. After generalizing the Fabry-Perot method to include driving ac fields, taking a double-barrier diode as an example, we will study the characteristic scaling parameter of single driven barriers more closely.

We denote the partial transmission (reflection) amplitude of a single driven barrier from channel j (i.e., with incident energy E_j) to channel l as $t_{lj}^{l,r}$ ($r_{lj}^{l,r}$), where the superscripts l, r indicate from which side the electron impinges on the barrier (see Fig. 1). The “optical” path across the quantum well of width d carries the phase factor $Q_{lj} = \delta_{lj}\exp(ik_l d)$ with $k_l = \sqrt{2m(E_0 + l\hbar\omega)}/\hbar$.¹⁷ The transmission amplitudes through the double-barrier diode for an electron incident from the left can be calculated by summing over all optical paths, resulting in a geometric series,

$$t = t^{2,l}(I + R + R^2 + \dots)Q t^{1,l} = t^{2,l}(I - R)^{-1}Q t^{1,l}, \quad (1)$$

with the kernel $R = Qr^{1,r}Qr^{2,l}$ describing one reflection cycle in the quantum well starting and ending at the left wall of the right barrier. Note that while in the static case R is a scalar,

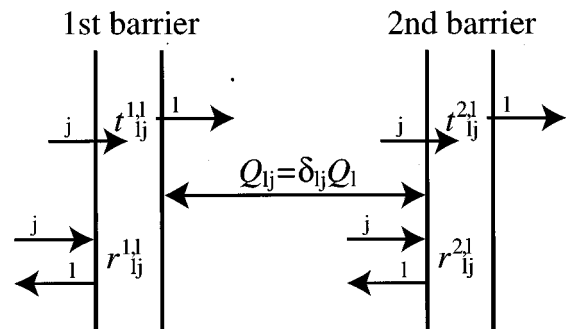


FIG. 1. Schematics of the notations used for the transmission and reflection amplitudes and the optical path Q that underlie the Fabry-Perot approach.

it is a matrix of infinite rank for finite ac driving. Similarly, the reflection amplitudes at the double barrier are found as

$$r = r^{l,l} + t^{l,r} Q r^{2,l} (I - R)^{-1} Q t^{l,l}. \quad (2)$$

This example shows how, in principle, the Fabry-Perot method can be employed to reduce the analysis of complex tunneling structures to that of single driven barriers. Let us therefore first discuss the scaling behavior of the sideband spectrum in single barriers. For simplicity, we consider an opaque δ -function barrier at the origin with static transmission and reflection amplitudes t_{dc} and r_{dc} , respectively.¹⁸ We assume that the photon energy is small compared to the incident energy, i.e., $v = \hbar\omega/E_0 \rightarrow 0$, so that all sidebands have the same wave vector k_0 and there is no disturbing effect from the conduction-band edge. On the left- (right-) hand side of the δ barrier, the ac driving potential is taken to be of the general form $V_{ac}(z,t) = (\hat{a}^{l,r}z + \hat{b}^{l,r})\cos\omega t$ with $\hat{a}^{l,r} = a^{l,r}m\omega^2/k_0$ and $\hat{b}^{l,r} = b^{l,r}\hbar\omega$. After matching the wave functions at the origin, the transmission amplitudes in the sidebands are found to obey the relation (for an electron incident from the left)

$$\sum_n t_n e^{-in\omega t} = t_{\text{dc}} \exp[i(a^r - a^l)\cos\omega t] \times \exp[i(b^r - b^l)\sin\omega t], \quad (3)$$

which has the solution

$$t_n = t_{\text{dc}} i^n J_n \left[\sqrt{(a^r - a^l)^2 + (b^r - b^l)^2} \right] \exp \left[in \arctan \left(\frac{b^r - b^l}{a^r - a^l} \right) \right]. \quad (4)$$

The reflection amplitudes, on the other hand, turn out not to depend at all on the ac potential on the other side of the barrier,

$$r_n = r_{\text{dc}} (-i)^n J_n(2a^l). \quad (5)$$

Equation (4) has a number of interesting limiting cases: For no driving on the left- and spatially uniform driving on the right-hand side, we recover the Tien-Gordon solution⁹ $t_n = t_{\text{dc}} J_n(-V_{ac}/\hbar\omega)$ and $r_n = r_{\text{dc}} \delta_{n0}$ with its ω^{-1} scaling behavior. By contrast, homogeneous driving with $eFz\cos\omega t$ on either side of the barrier yields $t_n = t_{\text{dc}} \delta_{n0}$ and $r_n = r_{\text{dc}} (-i)^n J_n(2eFk_0/m\omega^2)$, which shows the same ω^{-2} scaling as an ac field driven isolated quantum well.¹¹ Figure 2 illustrates the ‘‘numerically exact’’ results of a transfer-matrix calculation for this case, but using a barrier of finite height. It clearly shows the dominance of the $n=0$ channel in the transmission and the highly oscillatory behavior in reflection. The fact that $-t_n = t_{\text{dc}} \delta_{n0}$ is not strictly fulfilled in the exact solution is due to higher-order effects resulting from the scaled photon energy v being finite, which have been neglected in the approximate analytical solutions (4) and (5). Finally, if the driving ac field is *continuous* across the barrier, one finds $t_n = t_{\text{dc}} i^n J_n(a^r - a^l)$, and again $r_n = r_{\text{dc}} (-i)^n J_n(2a^l)$. As we shall discuss in more detail below, Eq. (4) also describes the *crossover* between the two scaling factors $b = V_{ac}/\hbar\omega$ and $a = eFk_0/m\omega^2$.

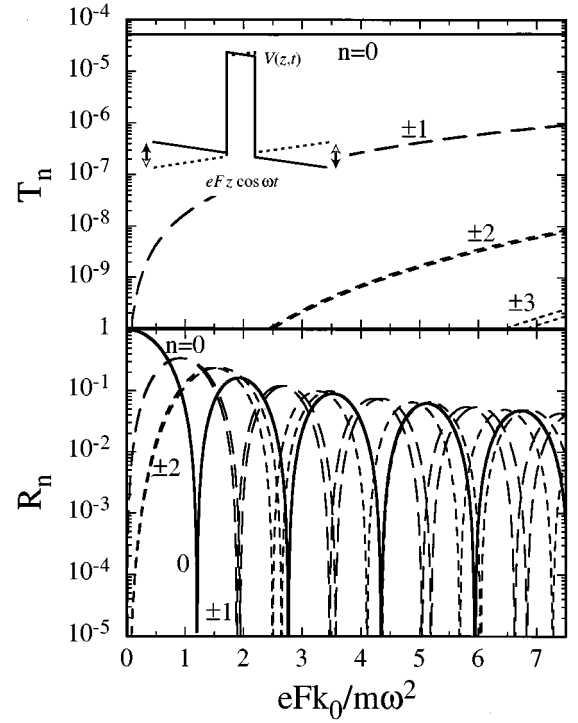


FIG. 2. Transmission and reflection probabilities $T_n = |t_n|^2 |k_n/k_0|$ and $R_n = |r_n|^2 |k_n/k_0|$ for a single barrier driven by $eFz\cos\omega t$ calculated using a transfer-matrix method. Transmission occurs mainly via the center band $n=0$, whereas an $eFk_0/m\omega^2$ scaling is seen in the reflection.

Note that in all cases the *total* transmission and reflection probabilities for a δ -function barrier are, respectively, given by $|t_{\text{dc}}|^2$ and $|r_{\text{dc}}|^2$, i.e., they *do not* depend on the ac potential to the lowest order in $v = \hbar\omega/E_0$. The requirement for any experimental verification of PAT through single barriers is therefore that *partial* transmission or reflection probabilities of individual sidebands be measured. Furthermore, knowing the polarization and spatial behavior of the ac potential is not only crucial for determining the characteristic scaling parameter ($V_{ac}/\hbar\omega$ versus $eFk_0/m\omega^2$), but also for deciding *how* to measure PAT: In a Tien-Gordon configuration, e.g., as realized in a tunnel junction between metals, it is best to measure the *transmitted* PAT electrons, while for a homogeneous ac field F across the barrier, one must monitor the *reflected* PAT electrons, since in this case, according to Eq. (4), all sidebands except for the center band vanish in transmission: $t_n = t_{\text{dc}} \delta_{n0}$.

To illustrate the dramatic effects that subtle changes in the ac driving potential can have, we now come back to the driven double-barrier diode and examine two special cases: In the first case, the driving ac field F is taken to be homogeneous across the entire structure, yielding an ac potential $V_{ac}(z,t) = eFz\cos\omega t$, while in the second case the ac field is assumed to be the same in the quantum well, but zero outside. Similar systems have also been studied using the tunneling Hamiltonian formalism,¹⁹ but without analyzing the ω dependence of PAT.

Assuming high, opaque barriers, we may use the transmission and reflection amplitudes of driven δ -function barriers, which with $V_{ac}(z,t) = eFz\cos\omega t$ and Eqs. (4) and (5) are given by

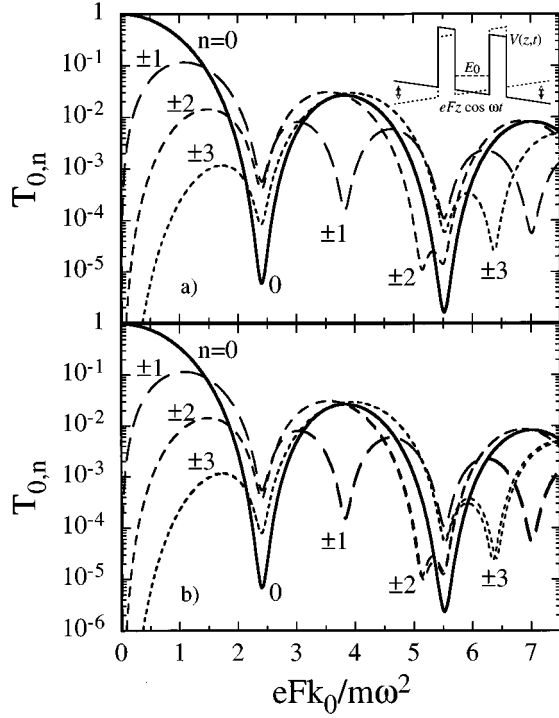


FIG. 3. Transmission probability in the lowest few sidebands through a driven double-barrier diode (see inset in top panel) as a function of driving strength for an incoming electron at the energy E_0 of the lowest resonance in the static quantum well: (a) Fabry Perot, (b) transfer-matrix method.

$$\begin{aligned} r_{ij}^{1,r} &= r_{dc}^{1,r} i^{l-j} J_{l-j}(2a), \\ r_{ij}^{2,l} &= r_{dc}^{2,l} (-i)^{l-j} J_{l-j}(2a), \\ t_{ij}^{1,2} &= t_{dc}^{1,2} \delta_{ij}. \end{aligned} \quad (6)$$

Here $a = eFk_0/m\omega^2$ with k_0 being the wave vector of the incident electron. The kernel R then becomes

$$\begin{aligned} R_{jl} &= r_{dc}^{1,r} r_{dc}^{2,l} \sum_n \exp(ik_j d) i^{j-l-n} J_{j-l-n}(2a) \\ &\quad \times \exp(ik_{l+n} d) (-i)^n J_n(2a). \end{aligned} \quad (7)$$

In the limit $v = \hbar\omega/E_0 \ll 1$ we can expand the wave vector of sideband l as $k_l = k_0 \sqrt{1 + lv} \approx k_0(1 + lv/2)$, allowing us to perform the sum analytically,

$$R_{jl} = r_{dc}^{1,r} r_{dc}^{2,l} e^{ik_0 d [2 + v(3j+l)/4]} J_{j-l}(|4a \sin(k_0 d v/4)|). \quad (8)$$

Using Eqs. (4), (6), and (8) we have plotted in Fig. 3(a) the transmission probabilities for tunneling through a driven symmetric double-barrier diode which display a $eFk_0/m\omega^2$ scaling behavior. For comparison, we also present in Fig. 3(b) the results of a calculation using transfer matrices. The agreement is excellent, with minor discrepancies appearing in the asymmetry of the ‘‘mirror’’ sidebands $\pm|n|$. Apart from being computationally faster by one or two orders of magnitude compared to the transfer-matrix method, a major virtue of the Fabry-Pérot approach lies in the fact that for generating Fig. 3(a) we have only used the dc transmission and reflection amplitudes of a single, undriven barrier. In

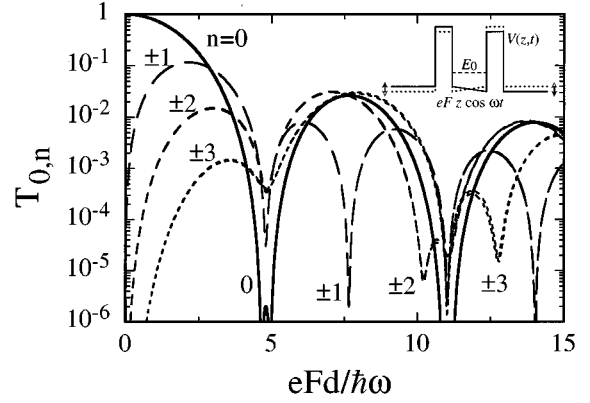


FIG. 4. Transmission probability as a function of the ac voltage drop across the quantum well for a double-barrier diode. In this case the ac driving potential increases *linearly* inside the quantum well as $eFz \cos \omega t$, while it is *flat* outside, $V_{ac}(|z| > d/2) = \pm eF(d/2) \cos \omega t$.

addition, it is more amenable to introducing a phase-breaking mechanism by randomizing the phase in the optical-path matrix Q traversing the quantum well.¹⁶

Now let us assume that the ac potential rises linearly in the quantum well, but is flat outside (see inset of Fig. 4),

$$V_{ac}(z,t) = \begin{cases} -eFd/2 \cos \omega t, & z < -d/2 \\ eFz \cos \omega t, & |z| \leq d/2 \\ eFd/2 \cos \omega t, & z > d/2. \end{cases} \quad (9)$$

One might think that the scaling parameter for this scenario is again $a = eFk_0/m\omega^2$, since this is the characteristic scaling found for the sideband amplitudes in an isolated quantum well driven by $eFz \cos \omega t$.¹¹ However, numerical analysis shows that for a driving potential of the form (9), the scaling parameter is $eFd/\hbar\omega$, which is of the Tien-Gordon type (see Fig. 4). The explanation for this result lies in the different transmission and reflection amplitudes through a single barrier in the two scenarios.

In both cases, the ac fields are the same *inside* the quantum well and, hence, according to Eq. (5), lead to the same reflection amplitudes at the *inner* walls of the barriers, resulting in identical kernels $R = Qr^{1,r}Qr^{2,l}$. Any difference, therefore, must arise from the different transmission amplitudes through the barriers. For homogeneous driving these are given by $t_n = t_{dc} \delta_{n0}$, while for a Tien-Gordon type of driving in the outside region with the ac potential being continuous across the barriers, one has $t_n = t_{dc} i^n J_n(a)$. The latter situation is thus characterized by an injection of the incident electron into *all* sidebands of the quantum-well resonance, weighted by the Bessel function factors, while in the former case injection occurs primarily into the center band only.²⁰ We conclude that even though the driven state in the quantum well, a Floquet state, is the same in both cases, a tunneling ‘‘spectroscopy’’ of this state yields different results depending on the behavior of the ac field in the *outside* regions. This result is at first somewhat counterintuitive, but finds its explanation in the observation that this spectroscopy is not done with a monochromatic energy but rather a series of energies $E_0 + n\hbar\omega$. Consequently, the nature of the driven

state in the quantum well with its ω^{-2} scaling behavior may be completely masked if the amplitudes of different channels interfere appropriately. Finally, with $v = \hbar\omega/E_0$, the two driving scales relate as $v \times eFk_0/m\omega^2 \sim eFd/\hbar\omega$, implying that for the same ac driving field F inside the quantum well the homogeneous driving is much more effective.

Let us briefly discuss the question under which conditions an ac driving potential $eFz \cos\omega t$, which diverges as $z \rightarrow \pm\infty$, is a realistic description for a particular device, and hence, whether the scaling parameter $eFk_0/m\omega^2$ can be observed experimentally. Evidently, a finite electric field that extends to a considerable distance beyond the tunnel barrier requires the screening length to be larger than the characteristic size of the device. Therefore, the carrier concentration in the outside regions should be low. Also, the ac field F should be constant over the phase coherence length of the electrons. Both of these constraints are within reach of today's technology.

The characteristic scaling parameters we have studied in this paper are the ones relevant for *transport*, as they are based on the analysis of transmission and reflection probabilities. It should be noted that the parameters characteristic for the *energy spectrum* of driven systems are, in general, different. For the ‘‘coherent destruction of tunneling’’ in a driven quartic quantum well one finds $\mu F/\hbar\omega$, where μ is the dipole moment between the two lowest states,²¹ while the ‘‘collapse of minibands’’ in a driven superlattice is governed by $eFd/\hbar\omega$, with d being the superlattice period.²² In fact,

the numerical analysis of a symmetric driven *double-well* tunneling diode reveals that while the photonic sidebands in the transmission probability exhibit a ω^{-2} scaling behavior, the tunnel splitting Δ of the two lowest states—as determined by the corresponding resonances in the total transmission probability as a function of energy—shows the typical $\Delta = \Delta_0 J_0(\mu F/\hbar\omega)$ dependence of a driven two-level system for $E_0 \gg \hbar\omega \gg \Delta_0$ and provided that higher-lying levels do not interfere.

In conclusion, we have used the Fabry-Perot method to reduce the problem of coherent transmission and reflection in complicated driven tunneling structures to that of single driven barriers. Assuming an ac potential of the general form $V_{ac}(z,t) = (\hat{a}^{l,r}z + \hat{b}^{l,r})\cos\omega t$ on either side of the barrier, we find an analytic expression for the characteristic scaling parameter of the photonic sidebands that exhibits a strong dependence on the spatial behavior of the ac potential, indicating that the Tien-Gordon theory is *not* applicable in experiments involving finite ac *fields* rather than flat ac *potentials*. While the former shows a ω^{-2} dependence, the latter varies as ω^{-1} .

One of us (M.W.) gratefully acknowledges the warm hospitality of Professor Kotthaus' group, in particular, D. Wharam, and is thankful for the scientific discourses he enjoyed during his stay in Munich. Discussions with C. Barnes are much appreciated. This work was supported by the Sonderforschungsbereich 348.

*Electronic address: wagner@phy.cam.ac.uk

¹F. Ehlitzky, *Can. J. Phys.* **59**, 1200 (1981); *ibid.* **63**, 907 (1985).

²R. A. Wyss, C. C. Eugster, J. A. del Alamo, and Q. Hu, *Appl. Phys. Lett.* **63**, 1522 (1993).

³L. P. Kouwenhoven *et al.*, *Phys. Rev. Lett.* **73**, 3443 (1994).

⁴R. H. Blick *et al.*, *Appl. Phys. Lett.* **67**, 3924 (1995).

⁵B. J. Keay *et al.*, *Phys. Rev. Lett.* **75**, 4102 (1995).

⁶S. Zeuner *et al.*, *Phys. Rev. B* **53**, R1717 (1996).

⁷K. Unterrainer *et al.*, *Phys. Rev. Lett.* **76**, 2973 (1996).

⁸T. C. L. G. Sollner *et al.*, *Appl. Phys. Lett.* **43**, 588 (1983).

⁹P. K. Tien and J. P. Gordon, *Phys. Rev.* **129**, 647 (1963).

¹⁰J. R. Tucker, *IEEE J. Quantum Electron.* **15**, 1234 (1979); J. R. Tucker and M. J. Feldman, *Rev. Mod. Phys.* **57**, 1055 (1985).

¹¹M. Wagner, *Phys. Rev. Lett.* **76**, 4010 (1996).

¹²B. Birnir, B. Galdrikian, R. Grauer, and M. Sherwin, *Phys. Rev. B* **47**, 6795 (1993).

¹³H. C. Liu, *Appl. Phys. Lett.* **52**, 453 (1988).

¹⁴M. Wagner, *Phys. Rev. B* **49**, 16 544 (1994); *Phys. Rev. A* **51**, 798 (1995).

¹⁵J. G. Platero and C. Tejedor, *Phys. Rev. B* **50**, 4581 (1994).

¹⁶Y. Hu, *J. Phys. C* **21**, L23 (1988).

¹⁷In general, Q contains a time-dependent phase factor, but since in the end we are interested in *probabilities* only, it is sufficient to evaluate Q ($t=0$).

¹⁸A driven δ -function barrier in a 1D Luttinger liquid was discussed in M. Sassetti, U. Weiss, and B. Kramer, *Solid State Commun.* **97**, 605 (1996); M. Sassetti and B. Kramer, *Phys. Rev. B* **54**, R5203 (1996).

¹⁹R. Aguado, J. ĩnarrea, and G. Platero, *Phys. Rev. B* **53**, 10 030 (1996).

²⁰We have checked the quality of these approximate transmission and reflection amplitudes by using the Fabry-Pérot approach to reproduce Figs. 3(b) and 4.

²¹F. Großmann, T. Dittrich, P. Jung, and P. Hänggi, *Phys. Rev. Lett.* **67**, 516 (1991).

²²M. Holthaus, *Phys. Rev. Lett.* **69**, 351 (1992).